Scilight

International Journal of Transportation and Logistics Research
https://www.sciltp.com/journals/ijtlr

Article

Check for updates

Tugboat Scheduling for Drop-and-Pull Transport in Inland Waterway Networks

Shibing Xiao and Xuan Qiu *

Department of Industrial Engineering and Decision Analytics, Hong Kong University of Science and Technology, Hong Kong
* Correspondence: xuanqiu@ust.hk

How To Cite: Xiao, S.; Qiu, X. Tugboat Scheduling for Drop-and-Pull Transport in Inland Waterway Networks. *International Journal of Transportation and Logistics Research* **2026**, *2*(1), 6. https://doi.org/10.53941/ijtlr.2026.100006

Received: 20 March 2026
Revised: 16 April 2026
Accepted: 28 April 2026
Published: 27 May 2026

Abstract: This paper studies a tugboat–barge scheduling problem in inland waterways where tugboats tow multiple barges and perform multiple trips under a drop-and-pull (DP) mode. We formulate a mixed-integer programming model that determines tug routes, barge assignments, and service times under time-window and capacity constraints, and propose an Adaptive Large Neighborhood Search (ALNS) algorithm with simulated annealing to solve practical-scale instances. A case study based on the middle–lower Yangtze trunk network and a short-distance regional network around Shanghai shows that long-distance DP transport exhibits a clear three-stage demand–cost pattern with route structures remaining stable up to a critical demand threshold, whereas short-distance transport on a compact network experiences frequent route reconfigurations and highly fluctuating cost elasticity. Sensitivity analyses further reveal a cost-driven switch between integrated trunk routing and more dispersed end-routing when barge unit costs become sufficiently higher than tugboat costs, offering guidance for fleet deployment and pricing in DP systems.

Keywords: tugboat; barge; drop-and-pull mode; ALNS; inland transport

1. Introduction

Barge transportation refers to the movement and delivery of goods using barges. A barge is a flat-bottomed vessel designed for transporting cargo on rivers, canals, and other inland waterways. It is typically used for bulk commodities such as coal, grain, oil, construction materials, and containers. A typical barge transportation process involves loading goods onto the barge at the origin, securing the cargo, and then transporting it to the destination via waterways. This mode is generally adopted in regions where inland waterway transport is cost-effective, and it is especially suitable for large and heavy goods, providing an alternative to road or rail transportation. In addition, barge transportation is often considered economical and environmentally friendly because, compared with other modes, it generally consumes less fuel and generates fewer emissions.

Barges usually require towing by tugboats. A tugboat-based system can be regarded as consisting of two parts: a motorized unit that can move independently (i.e., the tug boat) and a non-motorized unit that must be towed (i.e., the barge). Accordingly, barge transportation can be classified as operating under the Drop Pull (DP) mode. As il lustrated in Figure 1, in the DP mode, the motorized unit can be decoupled from the non-motorized unit. The barge is left at the customer's site for loading and unloading operations, while the tugboat departs to perform other transport tasks. Once loading and unloading are completed, the tugboat returns to tow the original barge away, or another tugboat may take over the barge. The separation and connection operations can be completed conveniently within a very short time.

In recent years, DP-based tug–barge systems have gained renewed importance in China and other countries due to tightening environmental regulations, "road-to-water" modal shift policies, and rising fuel and labor costs. Inland waterways such as the middle–lower Yangtze have become critical corridors for containerized and bulk cargo flows, where operators face the challenge of organizing high-frequency barge movements under stringent time-window constraints while 'controlling fleet operating costs. Despite this practical relevance, the integrated scheduling of tugboats and barges under a DP mode, with realistic time windows and network structures, remains relatively under-explored in the academic literature.

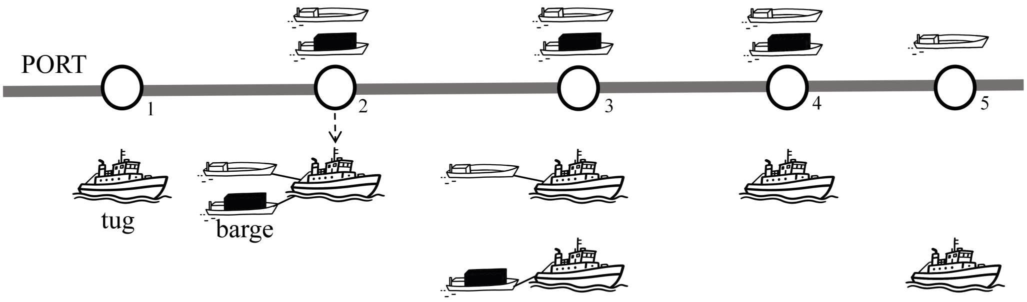

Figure 1. The Drop Pull Mode

This paper focuses on barge transportation under the DP mode and analyzes how total transportation costs vary with the shipping network scope, demand volume, and transportation cost parameters. By explicitly modeling tug–barge coordination and time-window-constrained demands on realistic inland waterway networks, we aim to bridge the gap between abstract vehicle-routing models and the operational realities of DP-based barge systems. The main findings are summarized as follows:

- Stability of optimal routes. Overall, the optimal route for long-distance trans portation is more stable than that for short-distance transportation. In both demand variation and cost-variation experiments, long-distance transport routes exhibit higher stability.
- Interaction between distance, demand, and cost. Transportation distance significantly affects the relationship between demand and total cost. In long distance transportation, shipping demand has a phased impact on total cost, and costs surge once demand exceeds a certain threshold. In contrast, in short-distance transportation, the impact of demand on cost weakens periodically and shows pro nounced fluctuations.
- Impact of unit cost changes. Changes in a single type of transportation cost are approximately linearly related to the total cost. Such changes rarely alter the optimal route choice. Only when the unit transportation cost of barges becomes significantly higher than that of tugboats does the routing strategy change to reduce costs, causing the total cost to deviate from linear behavior.

Motivated by these observations, this study pursues the following research objectives: (i) to develop a mixed-integer programming model that captures tugboat routes, barge flows, and time-window-constrained demands under a DP mode on realistic waterway networks; (ii) to design an efficient meta-heuristic based on Adaptive Large Neighborhood Search (ALNS) for solving practical-scale instances; and (iii) to quantify how demand volume, transportation distance, and cost parameters jointly shape optimal DP transport plans and to derive managerial implications for different types of inland waterway networks.

The remainder of this paper is organized as follows. Section 2 reviews the related literature from three perspectives. Section 3 formally describes the DP problem and presents the corresponding mathematical model. Section 4 introduces the solution approach and details the Adaptive Large Neighborhood Search (ALNS) algorithm employed. Section 5 conducts numerical experiments and provides analysis. Finally, Section 6 concludes the paper.

2. Literature Review

2.1. Tugboat Scheduling and Barge–Tug Operations

To date, although the application of tugboats in ports is widespread, studies on tugboat scheduling problems are still relatively scarce. Existing research mainly focuses on tugboat assignment and scheduling in seaports or river–sea transport systems, often under various operational uncertainties.

Wei et al. [1] address a real-life Tugboat Scheduling Problem (Tug-SP) in container ports. They formulate the Tug-SP as a mixed-integer linear programming (MILP) model and evaluate the proposed algorithm using real ship traffic data from the Port of Singapore. Kang et al. [2] consider a tugboat scheduling problem for large container ports, taking into account uncertainty in both container ship arrival times and tugging process durations.

From the perspective of joint barge–tug operations, Hao et al. [3] study a barge and tugboat joint scheduling problem arising from a river–sea intermodal transport system, where non-self-propelled barges travel with the help of tugboats between an inland river bulk port and sea transshipment platforms to transport cargo. Similarly, Zhen et al. [4] propose an exact algorithm based on Branch-and-Price to optimize the scheduling of seaport tugboats in inland barge transportation. Their model involves barge allocation and tugboat departure time decisions to minimize tugboat operating costs and delay penalties.

Considering modeling under uncertainty and heuristic solution approaches, Li et al. [5] propose a novel fuzzy programming optimization model and a customized Grey Wolf Optimization algorithm for tugboat scheduling under uncertainties. Comparative analysis and sensitivity validation show that their method achieves superior efficiency in minimizing fuel and delay costs. Jia et al. [6] construct an integer programming model for tugboat scheduling in busy seaports, considering berth plans, tug points, and horsepower requirements. They propose an iterative algorithm that combines Lagrangian relaxation and Benders decomposition, and validate it using real data from Shanghai container port, showing that the approach can efficiently generate near-optimal solutions.

Some studies formulate tugboat scheduling as complex task-scheduling problems and solve them via advanced meta-heuristics. Xu et al. [7] model tugboat scheduling as a multiprocessor task scheduling problem (MTSP), taking into account multi-anchorage bases and multi-stage operations. They propose a hybrid simulated annealing–ant colony algorithm to minimize total operation time, with computational experiments showing the sensitivity to shifting-berth operations and the benefits of timely tugboat returns. Sun et al. [8] address large-scale tugboat scheduling with cross-region constraints and uncertainties, and propose an improved genetic algorithm (GA-RE) with a task-triggered strategy for dynamic optimization. Simulation results at Zhoushan Port demonstrate that GA-RE outperforms both historical scheduling schemes and a standard genetic algorithm in terms of scalability and efficiency. Fan et al. [9] propose a two-stage mixed-integer linear programming model for the integrated optimization of port berth allocation and tugboat scheduling. By combining a genetic algorithm and a variable neighborhood search algorithm, they effectively reduce overall port operating costs.

Tug scheduling in inland waterways has also been investigated from a green logistics perspective. Zhu et al. [10] study tug scheduling for inland waterways, focusing on minimizing carbon emissions associated with inland waterway logistics. They introduce a mixed integer programming (MIP) model for tug scheduling that considers barge transshipment, which is similar to our study. However, the Drop-and-Pull (DP) mode is not factored in during their model development.

A number of recent works emphasize algorithmic enhancements for tugboat scheduling under complex, uncertain, and multi-objective conditions. Wang et al. [11] propose an Adaptive Large Neighborhood Search (ALNS) algorithm to solve a Tugboat Scheduling Problem with multiple services and multiple wharfs (Tug-SP-MSMW). It handles synchronous constraints through an efficient feasibility checking procedure and verifies the effectiveness of the algorithm in large-scale instances. Yao et al. [12] propose an Improved Grey Wolf Optimization (IGWO) algorithm for a multi-objective tugboat scheduling problem. By optimizing convergence parameters and update strategies, the performance of the algorithm is significantly improved and verified in a real-world port case. Ren et al. [13] propose a two-stage multi-criteria decision-making method that takes into account the reliability of the tugboat matching scheme. By integrating fuzzy mathematics and a Memetic algorithm, they optimize tugboat scheduling to reduce fuel costs and enhance reliability. The effectiveness of the method is verified through actual data from the Port of Guangzhou.

Overall, these studies provide an important methodological and empirical basis for tugboat scheduling and barge–tug operations. However, most of them do not explicitly consider the tugboat–barge DP mode with continuous sailing times, random initial positions, and highly stochastic time windows driven by natural conditions such as tides.

2.2. Vehicle Routing and Road-Based Drop-and-Pull Systems

From a methodological perspective, the tugboat DP problem studied in this paper is similar to the vehicle routing problem with pickup and delivery services in road transportation. Dumas et al. [14] propose an exact algorithm based on column generation and constrained shortest path to solve the Pickup and Delivery Problem with Time Windows (PDPTW). Their method handles multiple constraints through dynamic programming and achieves optimal scheduling for multiple depots and heterogeneous vehicle fleets.

Within the broader DP system literature, Li et al. [15] study a whole-process managed DP system, noting its recognized flexibility and cost advantages. They point out that China's DP market faces issues such as decentralization, non-standardization, and insufficient IT support. To address these problems, they design an IoT-integrated management system for real-time monitoring of personnel, cargo, and vehicles, aiming to enhance the overall logistics service level. Chen et al. [16] propose an optimized tractor scheduling method based on an improved ant colony algorithm in road drop-and-pull transportation, with the objective of minimizing the total cost of the DP system. Their experiments identify an optimal ratio of tractors to semi-trailers, and the optimized scheme significantly reduces costs.

Several studies further extend DP-related concepts into haulage and multi-trailer operations. Shiri et al. [17] propose an optimization model for haulage scheduling that takes into account time window constraints. By integrating the Reactive Tabu Search (RTS) algorithm, they solve a multi-depot Traveling Salesman Problem with Time Windows (m-TSPTW), and verify through experiments the impacts of truck reservation quotas, queuing times, and depot locations on haulage efficiency. Zhang et al. [18] model multi-trailer drop-and-pull container transportation as a nonlinear programming problem, exploring transportation routes and costs under varying trailer quantities using a 3-vector procedure for objective calculation and feasibility verification. Feng et al. [19] propose a two-stage truck–cargo model, first screening candidate vehicles for tasks and then forming truck alliances, and validate the effectiveness of collaborative scheduling via genetic algorithms.

These studies provide significant references for the establishment of tug DP models, especially the following two papers. Wang et al. [20] devise solutions for the Multi-Trip Multi-Trailer Drop-and-Pull Container Drayage Problem within truckload transportation operations, aimed at minimizing overall transportation costs. In their study, each tractor has the capacity to tow up to $K(\geq 2)$ trailers, operating in the DP mode, and the ALNS method is deployed to address the problem. Wang et al. [21] study the drop-and-pull container transportation problem considering drivers' mandatory rest (i.e., including the operation time windows of trailers). A mixed-integer programming model and a backtracking adaptive threshold acceptance algorithm are proposed, and their effectiveness is verified through experiments.

2.3. Differences and Contributions Relative to Existing DP Studies

Despite the valuable insights provided by the above DP-related studies, the tugboat DP problem investigated in this paper differs from them in several essential aspects.

First, in terms of model establishment, although the truck drop-and-pull transportation studies in [20,21] also adopt mixed-integer programming and take cost optimality as the objective, they do not fully consider the impact of time window constraints on the synergy of DP transportation. The tractor–trailer study in [21] introduces time window constraints, but its time windows are dominated by manual operational rules, and the scheduling strategy tends to be time-flexible. In contrast, the tugboat DP transportation problem studied in this paper has significantly different modeling characteristics: tugboat transportation time is more continuous; the starting positions of tugboats and barges are completely random without fixed base design; and the time windows are highly random due to natural conditions such as tides. These features make the scheduling strategy maintain strict time rigidity and significantly increase the complexity of feasible-solution construction.

Second, in terms of solution methods, although heuristic or meta-heuristic algorithms are widely used [11,20,21], this paper innovatively combines the ALNS algorithm with a simulated annealing framework. By optimizing the traditional "destruction–repair" operators and introducing a roulette wheel selection mechanism, the adaptability of the algorithm in large-scale scheduling problems is significantly improved. In contrast, the backtracking adaptive threshold acceptance algorithm used in [21] shows obvious disadvantages in computational efficiency, especially for large-scale instances.

Third, in terms of research focus, Wang et al. [20] mainly focus on the economic comparison between multi-trailer and single-trailer modes, while [21] emphasize flexible scheduling optimization considering drivers' rest time. This paper, however, pioneeringly conducts a systematic analysis of the differentiated impact mechanisms of multiple factors—such as transportation distance, demand scale, and cost structure—on the cost of tugboat DP transportation in two typical networks of inland waterways and coastal waterways, providing a brand-new decision-making perspective for transportation resource allocation in different water environments.

These innovations enable this study to surpass existing work in terms of problem complexity, algorithm applicability, and practical application value. At the same time, the above literature review highlights a clear research gap: existing studies on tugboat scheduling and drop-and-pull systems either abstract away from realistic DP tug–barge coordination with continuous sailing times and stochastic time windows, or they focus on road-based tractor–trailer operations. Empirical applications on realistic inland waterway networks with explicit time-window demands and systematic sensitivity analysis of demand, distance, and cost parameters are still scarce. Our work addresses this gap by combining a detailed DP tug–barge model with a scalable ALNS approach and by using two case studies on the Yangtze River system to link optimization results to managerial insights for maritime stakeholders.

3. Model Formulation

3.1. Problem Description

We consider a hinterland transport operator who manages a set of tugboats $P = \{1, \ldots, |P|\}$ and a set of barges $B = \{1, \ldots, |B|\}$ to serve container transport demands in an inland waterway network with multiple ports.

The transport network is represented by a directed graph $G = (N, A)$, where each node $i \in N$ is a seaport or inland port and each arc $(i, j) \in A$ denotes a feasible sailing leg from port i to port j.

A transport demand $d \in D = \{1, \ldots, |D|\}$ requests that a barge be towed from an origin port $S(d) \in N$ to a destination port $W(d) \in N$. We assume that demands are known in advance within a planning horizon $[0, T]$. For each demand d, the loading (pickup) operation at $S(d)$ must start within the time window $[\bar{E}_d^P, \bar{L}_d^P]$, and the barge must arrive at the destination port $W(d)$ within the delivery window $[\bar{E}_d^D, \bar{L}_d^D]$.

Under the drop-and-pull (DP) mode, a tugboat can decouple from a barge during loading/unloading and use the released time to serve other demands. Consequently, the tugboat that picks up a loaded barge at $S(d)$ may be different from the tugboat that later pulls the empty barge away from $W(d)$. We assume that coupling and decoupling times are negligible compared with sailing times, but waiting times at ports are explicitly modeled.

At the beginning of the planning horizon, each tugboat $p \in P$ is located at a known port $L(p) \in N$ and is available for operation. Barges are either idle at some port or already engaged in loading/unloading. For barge $b \in B$, its initial location is denoted by $L(b) \in N$. The sailing time of a tugboat from port i to port j is denoted by t_{ij} (hours). Each tugboat p can tow at most K_p barges simultaneously.

The objective of the tugboat scheduling problem is to construct sailing routes for all tugboats, assign demands and barges to these routes, and determine service times at ports such that all demands are satisfied within their time windows and all tugboat capacity constraints are respected, while minimizing the total operating cost of the operator.

3.2. Notation

Table 1 summarizes the notation used in the mathematical model.

Table 1. Sets, parameters, and decision variables.

Sets	
P	set of tugboats, indexed by p
B	set of barges, indexed by b
N	set of ports, indexed by i, j
$A \subseteq N \times N$	set of directed sailing arcs (i, j)
D	set of transport demands, indexed by d
Parameters	
T	length of the planning horizon
t_{ij}	sailing time from port i to port j, for all $(i, j) \in A$
C_p^T	operating cost per unit time of tugboat p
C_{ij}^B	transportation cost of one barge from port i to port j
K_p	towing capacity (maximum number of barges) of tugboat p
$L(p)$	initial port of tugboat p
$L(b)$	initial port of barge b
$S(d)$	origin port of demand d
$W(d)$	destination port of demand d
$[\bar{E}_d^P, \bar{L}_d^P]$	pickup time window of demand d at port $S(d)$
$[\bar{E}_d^D, \bar{L}_d^D]$	delivery time window of demand d at port $W(d)$
M	a sufficiently large positive constant
Decision variables	
$x_{ij}^p \in \{0, 1\}$	$x_{ij}^p = 1$ if tugboat p sails directly from port i to port j, and 0 otherwise
$q_{ij}^p \in \mathbb{Z}_+$	number of barges towed by tugboat p when departing from port i to port j
$y_d^p \in \{0, 1\}$	$y_d^p = 1$ if demand d is assigned to tugboat p, and 0 otherwise
$a_i^p \geq 0$	arrival time of tugboat p at port i (if it visits i)
$s_i^p \geq 0$	waiting time of tugboat p at port i before departure
$z_d^P, z_d^D \in \{0, 1\}$	auxiliary variables indicating whether the barge associated with demand d is picked up at $S(d)$ and dropped at $W(d)$, respectively

For clarity of exposition, the model is written at the tugboat–port level. The link between barge flows and tugboat routes is captured through the variables q_{ij}^p, z_d^P, and z_d^D.

3.3. Mathematical Modeling

The total cost consists of tugboat operating costs (sailing plus waiting) and barge transportation costs along all sailed arcs:

$$\min Z = \sum_{p \in P} C_p^T \left(\sum_{i \in N} s_i^p + \sum_{(i,j) \in A} t_{ij} x_{ij}^p \right) + \sum_{p \in P} \sum_{(i,j) \in A} C_{ij}^B \, q_{ij}^p. \tag{1}$$

3.3.1. Tugboat Route Continuity

Each tugboat starts from its initial port and either remains idle or follows a continuous path on G. For each tugboat $p \in P$,

$$\sum_{j:(L(p),j) \in A} x_{L(p)j}^p \leq 1, \qquad \forall p \in P, \tag{2}$$

$$\sum_{j:(i,j) \in A} x_{ij}^p - \sum_{j:(j,i) \in A} x_{ji}^p = 0, \qquad \forall p \in P, \, \forall i \in N \setminus \{L(p)\}, \tag{3}$$

which enforce flow conservation at intermediate ports and prevent branching; every visited port has exactly one predecessor and one successor on the route of tugboat p.

3.3.2. Demand Assignment

Each demand is served by exactly one tugboat:

$$\sum_{p \in P} y_d^p = 1, \qquad \forall d \in D. \tag{4}$$

If demand d is assigned to tugboat p, then tugboat p must visit both its origin port $S(d)$ and destination port $W(d)$:

$$y_d^p \leq \sum_{j:(S(d),j) \in A} x_{S(d)j}^p, \qquad \forall d \in D, \, \forall p \in P, \tag{5}$$

$$y_d^p \leq \sum_{j:(j,W(d)) \in A} x_{jW(d)}^p, \qquad \forall d \in D, \, \forall p \in P. \tag{6}$$

Variables z_d^P and z_d^D link barge pickup and drop decisions with demand assignment:

$$z_d^P = z_d^D = \sum_{p \in P} y_d^p, \qquad \forall d \in D. \tag{7}$$

Thus, for each demand, exactly one pickup and one drop operation will be performed in the network.

3.3.3. Barge Flow and Capacity Constraints

The number of barges carried by tugboat p when departing each port is updated according to pickup and drop decisions along the route. For each tugboat $p \in P$ and port $i \in N$,

$$\sum_{j:(i,j) \in A} q_{ij}^p - \sum_{j:(j,i) \in A} q_{ji}^p = \sum_{d \in D: S(d)=i} z_d^P - \sum_{d \in D: W(d)=i} z_d^D, \qquad \forall p \in P, \, \forall i \in N, \tag{8}$$

$$0 \leq q_{ij}^p \leq K_p \, x_{ij}^p, \qquad \forall p \in P, \, \forall (i,j) \in A. \tag{9}$$

Equation (8) conserves the number of barges on each tugboat route, while (9) restricts the number of towed barges on each arc to the capacity K_p.

3.3.4. Time Propagation and Time Windows

For any arc $(i,j) \in A$ sailed by tugboat p, its arrival time at port j must be consistent with the departure time from i. Using a big-M formulation:

$$a_j^p \geq a_i^p + s_i^p + t_{ij} - M\,(1 - x_{ij}^p), \qquad \forall p \in P, \, \forall (i,j) \in A. \tag{10}$$

For the initial port of tugboat p, we set

$$a^p_{L(p)} = 0, \qquad \forall p \in P. \tag{11}$$

If tugboat p serves demand d, its arrival time at the origin and destination ports must lie within the respective time windows:

$$\bar{E}^P_d \le a^p_{S(d)} \le \bar{L}^P_d + M\,(1 - y^p_d), \qquad \forall d \in D,\ \forall p \in P, \tag{12}$$

$$\bar{E}^D_d \le a^p_{W(d)} \le \bar{L}^D_d + M\,(1 - y^p_d), \qquad \forall d \in D,\ \forall p \in P. \tag{13}$$

When $y^p_d = 1$, these inequalities reduce to standard time-window constraints; when $y^p_d = 0$, they are relaxed. All arrival and waiting times are nonnegative:

$$a^p_i \ge 0, \quad s^p_i \ge 0, \qquad \forall p \in P,\ \forall i \in N. \tag{14}$$

The above model constitutes a coherent mixed-integer programming formulation that explicitly captures tugboat route continuity, barge flows, capacity constraints, and demand time windows under the DP mode.

4. Solution Method

4.1. An ALNS Algorithm Framework

Algorithmically, we design a hybrid Adaptive Large Neighborhood Search (ALNS) algorithm embedded in a simulated annealing (SA) framework to solve the proposed MIP for practical-size instances. The algorithm iteratively removes and reinserts parts of the current solution using several destroy and repair operators. Operator selection is controlled by adaptive weights updated according to historical performance.

Following [22], ALNS exhibits dynamic adaptability and strong local search capabilities: by gradually destroying and reconstructing local structures of solutions, it enables refined searches near high-quality solutions while avoiding premature convergence. Its extensibility facilitates integration with other heuristics such as SA to form hybrid strategies.

We select ALNS as the core meta-heuristic for two main reasons. First, the proposed tugboat–barge scheduling problem is a large-scale time-window routing/scheduling model with many binary routing and assignment variables, for which exact solvers quickly face scalability issues when the number of ports, tugboats, and demands grows. ALNS has proven effective for structurally similar vehicle-routing and maritime scheduling problems, offering a good trade-off between solution quality and computation time. Second, the destroy–repair framework is well suited to the DP setting, where complex interactions between tug routes, barge flows, and time windows can be handled by customized operators and a dedicated feasibility-checking procedure. Embedding ALNS in a simulated annealing framework further enhances its ability to escape poor local minima and explore diverse routing patterns.

Given a solution S, we define its cost by evaluating the objective function of the MIP (see Equation (1)):

$$\mathrm{Cost}(S) = \sum_{p \in P} C^T_p \left(\sum_{i \in N} s^p_i + \sum_{(i,j) \in A} t_{ij} x^p_{ij} \right) + \sum_{p \in P} \sum_{(i,j) \in A} C^B_{ij}\, q^p_{ij}. \tag{15}$$

A solution is feasible if it satisfies all flow, capacity, and time-window constraints of the model; feasibility is verified by a dedicated procedure described in Section 4.4.

The pseudo-code of the main ALNS–SA framework is given in Algorithm 1.

In Algorithm 1, lines 1–2 establish the SA framework, lines 3–6 select and apply destroy/repair, greedy, or random operators according to a roulette-wheel mechanism based on adaptive weights, lines 7–17 evaluate the new solution and update the current and best solutions under the SA acceptance criterion, and lines 18–19 implement operator-weight updates and the cooling schedule. The operator weights are updated using a standard ALNS reward scheme (e.g., [22]), so that operators that frequently lead to improved solutions receive higher selection probabilities in subsequent iterations.

Algorithm 1 Adaptive large neighborhood search with simulated annealing.

Input: Initial feasible solution S_0
Output: Best solution S_{best}

$S_{\text{curr}} \leftarrow S_0,\ S_{\text{best}} \leftarrow S_0$
$T \leftarrow T_{\text{init}}$ ▷ initial temperature
for iter $= 1$ **to** $Iter_{\max}$ **do**
  Select an operator op from { destroy–repair, greedy, random }
    according to roulette-wheel probabilities proportional to weights w_{op}
  Generate a neighbor S_{new} by applying op to S_{curr}
  if IsFeasible(S_{new}) **then**
    $\Delta \leftarrow \text{Cost}(S_{\text{new}}) - \text{Cost}(S_{\text{curr}})$
    if $\Delta \leq 0$ **or** $\text{rand}(0,1) < \exp(-\Delta/T)$ **then**
      $S_{\text{curr}} \leftarrow S_{\text{new}}$
      if $\text{Cost}(S_{\text{new}}) < \text{Cost}(S_{\text{best}})$ **then**
        $S_{\text{best}} \leftarrow S_{\text{new}}$
        UpdateWeight(op, reward_high)
      else
        UpdateWeight(op, reward_low)
      end if
    else
      UpdateWeight(op, reward_zero)
    end if
  end if
  $T \leftarrow \alpha T$ ▷ cooling factor $0 < \alpha < 1$
end for
return S_{best}

4.2. Initial Solution Generation

The combinatorial complexity of the problem grows quickly with the number of ports, tugboats, and demands. To efficiently provide a starting point for the ALNS, we design a three-step constructive heuristic that produces a feasible solution with very low computational overhead.

Step 1: Randomized demand–tug assignment.

Each demand $d \in D$ is tentatively assigned to a tugboat $p \in P$ drawn uniformly at random among those whose current load is below K_p. This yields a provisional one-to-one mapping between demands and tugboats.

Step 2: Route sequencing by temporal precedence.

For each tugboat p, we construct a route that visits the origins and destinations of its assigned demands in non-decreasing order of their earliest time windows (pickup and delivery). When conflicts occur (e.g., overlapping time windows or long detours), we insert short waiting times at intermediate ports or swap the order of two consecutive tasks if this reduces tardiness. This step guarantees a temporally consistent visiting sequence for each tugboat.

Step 3: Feasibility repair.

Using the feasibility-checking procedure of Section 4.4, we iteratively adjust the preliminary routes. If a capacity or time-window violation is detected for a tugboat p, one of its assigned demands is reallocated to another tugboat p' with sufficient remaining capacity and time slack, and the route of p' is re-sequenced accordingly.

The above construction has empirical complexity $\mathcal{O}(|D| \log |D|)$ due to the sorting operations in Step 2 and consumes less than a few percent of the total running time in our numerical experiments. Its main purpose is to provide a reasonably good and fully feasible initial solution for ALNS rather than to optimize the objective value.

The pseudo-code of the initial-solution generation procedure is given in Algorithm 2.

Algorithm 2 Initial solution construction.

Input: Demand set D, tugboats P, ports N
Output: Initial feasible solution S_0
1: **function** ConstructInitialSolution(D, P, N)
2: Initialize assignment map $\mathcal{A} \leftarrow \emptyset$ ▷ demand → tugboat
3: **for all** $d \in D$ **do**
4: Select $p \in P$ uniformly at random with current load $< K_p$
5: $\mathcal{A}(d) \leftarrow p$
6: **end for**
7: Initialize routes for all $p \in P$
8: **for all** $p \in P$ **do**
9: Let $D_p \leftarrow \{d \in D \mid \mathcal{A}(d) = p\}$
10: Sort D_p by non-decreasing earliest time windows (pickup/delivery)
11: Build a route for p visiting $S(d)$ and $W(d)$ for all $d \in D_p$ in the sorted order, inserting waiting times if needed
12: **end for**
13: $S_0 \leftarrow$ solution induced by routes of all $p \in P$
14: **while** IsInfeasible(S_0) **do**
15: Identify a violating tugboat p and a conflicting demand d
16: Select another tugboat $p' \in P$ with sufficient slack
17: Reassign d from p to p' and re-sequence the route of p'
18: Update S_0
19: **end while**
20: **return** S_0
21: **end function**

In Algorithm 2, lines 1–5 randomly allocate demands to tugboats, lines 6–11 construct time-consistent routes by temporal precedence, and lines 12–18 iteratively repair any capacity or time-window violations until a feasible initial solution is obtained.

4.3. Operators Design

The proposed ALNS algorithm starts from the initial feasible solution constructed in Section 4.2, which is regarded as both the current solution and the best solution found so far. By applying the SA framework to control the number of iterations, the algorithm seeks to obtain better solutions. In each iteration, the algorithm selects one of three types of operators—a cost-based destroy–repair operator, a deterministic greedy local-improvement operator, or a random perturbation operator—via a dynamically adjusted, weight-based roulette-wheel mechanism.

4.3.1. Worst-Removal Destroy Operator

The destroy operator implements a worst-removal strategy. For any feasible solution S, we first compute the cost contribution of each tugboat route:

$$\mathrm{RouteCost}(p, S) = C_p^T \left(\sum_{i \in N} s_i^p + \sum_{(i,j) \in A} t_{ij} x_{ij}^p \right) + \sum_{(i,j) \in A} C_{ij}^B \, q_{ij}^p. \tag{16}$$

We then rank tugboats in descending order of $\mathrm{RouteCost}(p, S)$. Let $\rho \in (0, 1]$ be the removal rate. The destroy operator selects the top $\lceil \rho |P| \rceil$ high-cost tugboats and removes all demands currently served by these tugboats from the solution, while keeping the routes of the remaining tugboats unchanged.

The worst-removal destroy operator is summarized in Algorithm 3.

By focusing on the most expensive routes, this operator dismantles inefficient parts of the solution and encourages better utilization of the tugboat fleet capacity.

Algorithm 3 Worst-removal destroy operator.

```
Input: Current solution S
Output: Partially destroyed solution S_d
function DESTROY(S)
    for all p ∈ P do
        cost[p] ← RouteCost(p, S)
    end for
    Sort P in descending order of cost[p]
    Let P_worst be the first ⌈ρ|P|⌉ tugboats in the sorted list
    S_d ← copy of S
    for all p ∈ P_worst do
        Remove all demands assigned to p from S_d
        Delete the corresponding visits from the route of p in S_d
    end for
    return S_d
end function
```

4.3.2. Cost-Based Repair Operator

Starting from a partially destroyed solution S_d, the repair operator reinserts all removed demands one by one. For each unassigned demand d, we evaluate all feasible insertion positions for every tugboat route and select the one with the minimum incremental cost.

Let $S_d \oplus (d, p, \mathrm{pos})$ denote the solution obtained by inserting demand d into the route of tugboat p at position "pos" (between two consecutive ports), with times updated by forward propagation. The incremental cost of this insertion is

$$\Delta\mathrm{Cost}(d, p, \mathrm{pos}) = \mathrm{Cost}\big(S_d \oplus (d, p, \mathrm{pos})\big) - \mathrm{Cost}(S_d). \tag{17}$$

The repair operator chooses, among all feasible insertions that satisfy capacity and time-window constraints, the one with the smallest $\Delta\mathrm{Cost}$.

The pseudo-code of the cost-based repair operator is given in Algorithm 4.

Algorithm 4 Cost-based repair operator.

```
Input: Partially destroyed solution S_d
Output: Repaired feasible solution S_r
function REPAIR(S_d)
    S_r ← S_d
    Let U be the set of unassigned demands in S_r
    while U ≠ ∅ do
        Select a demand d ∈ U (e.g., at random or by largest time window)
        best_Δ ← +∞, best_move ← null
        for all p ∈ P do
            for all feasible insertion positions pos in route of p do
                if insertion (d, p, pos) satisfies capacity and time windows then
                    Δ ← ΔCost(d, p, pos)
                    if Δ < best_Δ then
                        best_Δ ← Δ
                        best_move ← (d, p, pos)
                    end if
                end if
            end for
        end for
        Apply best_move to S_r and update route and timing of the corresponding tugboat
        Remove d from U
    end while
    return S_r
end function
```

This operator realizes precisely the statement “reassign demands to the lowest-cost transportation route”: the quantity being minimized is exactly the MIP objective in (15), and feasibility is enforced explicitly through capacity and time-window checks.

4.3.3. Greedy and Random Operators

The greedy operator performs local improvements on existing routes. For each tugboat p, it attempts pairwise swaps of consecutive visits and short reinsertions of ports within the route. If a modification yields a feasible solution with a strictly lower total cost, it is accepted; otherwise it is discarded. This process is repeated until no improving move can be found or a preset iteration limit is reached.

The random operator selects a tugboat at random, deletes a short subsequence of consecutive ports from its route, and reinserts the associated demands into randomly chosen feasible positions on other routes. This operator helps diversify the search and avoids premature convergence to poor local minima.

4.4. Feasibility Judgment

The solution optimized by the operators is considered feasible only when it satisfies the path constraints, time window constraints, and capacity constraints simultaneously. Before calculating the minimum cost objective value, the feasibility of the solution is usually verified to save computing power. The path constraints are mainly set according to the flow constraints in the network [18]. It is necessary to ensure that the path generated by this solution does not fork and is unique. At the same time, it is also necessary to ensure that the tugboat in the route will not pass through the same directed arc repeatedly, which may affect the experimental results. When the generated path is obviously inconsistent with the actual situation, the solution will be judged as infeasible.

The time window constraints set limitations based on the arrival time at the port calculated according to the path generated for each tugboat in each solution. In this constraint, first, it is necessary to determine which assignments are allocated to each tugboat, so as to obtain the time window range within which each tugboat should arrive at the port. Finally, compare whether the actual arrival time exceeds the time range. For some ports that may be passed through repeatedly, the transportation demand that should be completed at this port will be determined by identifying the paths before and after it, and then the time window judgment will be carried out.

The capacity constraint means that the number of barges towed by each tugboat is limited. When counting the number of lifting and lowering of barges by the tugboat, it is necessary to ensure that the loading capacity of the tugboat is non-negative and less than the maximum loading capacity of the tugboat. To implement this constraint, it is necessary to first establish the transportation path of the tugboat according to the task assignment. Secondly, calculate the barge loading capacity when the tugboat arrives at each port. Once the loading capacity exceeds the limited range, it is judged that the condition is not met and the solution is infeasible.

Now, if the solution passes these tests, it will be compared with the current solution saved in the system as a feasible solution. Finally, through repeated iterations, the algorithm will complete the process of finding the optimal solution with the ALNS as the framework.

4.5. Parameter Settings and Reliability

For completeness, we briefly report the main parameter settings of the ALNS–SA algorithm. The simulated annealing framework starts from a relatively high initial temperature and uses a geometric cooling schedule with factor $\alpha = 0.98$, so that uphill moves are frequently accepted at the beginning and gradually suppressed as the search progresses. The removal rate in the worst-removal operator is drawn from a small interval (e.g., $[0.1, 0.3]$) to balance intensification and diversification, and the maximum number of iterations and time limit are chosen so that the solution time does not exceed 60 seconds for the benchmark and case-study instances. As shown in Section 5.1, on instances where CPLEX proves optimality, ALNS–SA systematically finds solutions with objective values equal or very close to the optimum, and on larger instances it remains within about 0.5% of CPLEX’s best incumbent while using much less CPU time, which indicates a good level of reliability and robustness of the proposed approach.

5. Numerical Experiments

This study consists of two comparative analyses. The first section evaluates the performance of the Adaptive Large Neighborhood Search (ALNS) algorithm against the Mixed-Integer Linear Programming (MILP) solver CPLEX 12.10 through benchmark instances. The second section conducts a real-world case study to derive optimal solutions using ALNS, culminating in practical recommendations. All algorithms were implemented in Python 3.10, with experiments conducted on a desktop computer equipped with an Intel Core 2.50 GHz processor and 16 GB RAM. Through comprehensive computational experiments and sensitivity analyses, this paper demonstrates

ALNS's superior solution quality and computational efficiency in solving large-scale waterway tugboat routing problems with time windows, while providing actionable insights for logistics enterprises to optimize their tugboats deployment strategies.

5.1. Verification of ALNS Algorithm

To validate the effectiveness of the ALNS algorithm in solving tugboat scheduling problems, we constructed 20 test instances, collectively referred to as E. Each instance was designed with 3–5 port nodes (denoted as N) and 5 to 20 tugboats (denoted as n_p) to compare the capacity of the CPLEX and ALNS algorithm on different scales. Port coordinates were randomly generated within the geographical range of [longitude 105°–121°, latitude 28°–31°] which is close to the position of the Yangtze River segments and more convenient to the subsequence research. Tugboats were initially randomly distributed near ports, with transportation distances ignored. Transportation demand parameters were generated stochastically with time windows.

For most instances mentioned above, CPLEX can obtain optimal solutions within a reasonable time frame, so we conducted a comparative analysis by solving these instances with CPLEX and the ALNS algorithm. The experimental results are summarized in the table below.

All instances were solved by CPLEX 12.10 using its Python API. Unless otherwise stated, CPLEX was run with default settings, a relative MIP optimality gap (mipgap) of 10^{-4}, and a time limit of 7200 s. For instances 1–15, CPLEX terminated with status "optimal" and a reported relative gap of 0; therefore the corresponding objective values in Table 2 are proven global optima. The running times for these small instances are typically below 2 s, indicating that they are relatively easy for an exact solver.

For instances 16–20, the number of binary routing variables grows rapidly with the number of demands and tugboats. CPLEX reached the 7200-s time limit without closing the optimality gap; only the best incumbent objective values are reported in Table 2. In contrast, ALNS consistently produced high-quality feasible solutions within 60 s for all instances. For cases 16–20, the best solution found by ALNS is on average within 0.5% of the best incumbent of CPLEX, but with two orders of magnitude shorter running time, highlighting the advantage of the proposed meta-heuristic in large-scale settings.

Table 2. Comparison between the solution of and CPLEX and ALNS.

E	Port	Tug-Dem	Model by CPLEX		Model by ALNS		Gap
			OBJ	Time(s)	OBJ	Time(s)	
1	3	5–20	689.0	2.01	689.0	1.60	0.00%
2	3		822.0	1.57	822.0	1.24	0.00%
3	4		1274.9	1.54	1279.8	1.74	0.38%
4	4		1206.9	2.10	1206.9	2.23	0.00%
5	5		1259.7	2.23	1262.2	5.02	0.20%
6	3	10–40	1118.7	11.91	1118.7	6.86	0.00%
7	3		1180.8	11.44	1189.2	9.37	0.71%
8	4		1590.2	12.67	1590.2	10.46	0.00%
9	4		1669.0	12.03	1669.0	12.89	0.00%
10	5		1652.5	9.81	1656.8	14.33	0.26%
11	3	15–60	1675.1	43.50	1690.2	16.83	0.90%
12	3		1615.8	105.99	1618.8	21.69	0.19%
13	4		1936.5	397.12	1938.8	25.48	0.12%
14	4		2160.8	400.70	2160.8	15.64	0.00%
15	5		2219.8	582.24	2232.7	41.61	0.58%
16	3	20–80	2354.6	6614.627	2362.2	20.05	0.32%
17	3		——	>7200	2512.7	26.29	——
18	4		——	>7200	3161.2	40.46	——
19	4		——	>7200	2749.7	53.23	——
20	5		——	>7200	2883.9	54.82	——

5.2. Case Study of Long-Distance Shipping

Data description for the trunk-line case study. The long-distance case study is based on the middle–lower Yangtze trunk line reported in the China Port Yearbook (2023 Edition) [23]. We consider eight major container ports along this section: Shanghai, Nantong, Zhangjiagang, Taicang, Nanjing, Anqing, Jiujiang, and Wuhan. The pairwise sailing distances between these ports are obtained from the official river mileage tables in the Yearbook, and sailing times t_{ij} are calculated by dividing the distances by the average convoy speed used by local operators (approximately 17–19 km/h depending on the river segment). Under these assumptions, the distance between Shanghai and Wuhan corresponds to a sailing time of about 42 h for tug–barge convoys, which is consistent with industry practice on this route.

The planning horizon for the trunk-line case is set to one week ($T = 168$ h). For each demand d, the start of its pickup time window $\bar{E}_d^P$ is sampled uniformly from $[0, T - w_d]$, where the window width w_d is drawn from a uniform distribution between 6 and 24 h. The corresponding delivery window $[\bar{E}_d^D, \bar{L}_d^D]$ is generated by adding the expected sailing time between $S(d)$ and $W(d)$ plus a slack uniformly distributed between 4 and 12 h. This procedure yields time windows that are "uniformly spread" over the cycle in a statistically precise sense and reflects the variability of actual barge loading and unloading schedules.

Regulatory constraints and cost parameters are calibrated from current practice on the Yangtze River. In compliance with navigation regulations, the number of barges towed by a single tugboat should not exceed 4 vessels in the middle reaches and 6 vessels in the lower reaches. To simplify the model while retaining realism, we set the unified towing capacity to 5 barges per tugboat. Cost parameters are derived from actual transportation economics: the base operating cost for a tugboat is set to CNY 6000 per hour (with a plausible range of CNY 3000–7000 per hour in sensitivity analysis), and the additional cost for a barge is set to CNY 3000 per hour (with a range of CNY 2000–5000 per hour). This configuration balances fidelity to real operations with analytical tractability for systematic optimization.

In this case study, there are many primary variables influencing the optimal cost of drop-and-pull transport. To investigate their relationships with the optimal cost, we conduct the following sensitivity analysis.

5.2.1. Impact of Demands

The impact of transportation demand volume exerts a significant impact on operational cost structures. Suppose under fixed maritime resource conditions (maximum number of tugboats is 35), using a baseline demand of 140 shipment units, we implemented a systematic demand variation protocol with 7-unit perturbations per experimental run across 10 treatment groups. The time windows for the transportation demands are uniformly distributed within the cycle, and the time windows of newly added transportation demands are generated randomly.

We use Cost and ε to describe these experiments. The Cost column records the total cost at this demand level. ε refers to the cost elasticity, which can be used to determine the impact of the growth in transportation demand on the total cost and it is calculated as the cost change rate divided by demand volume change rate. According to economic theory [24], when ε is less than 1, there is an economy of scale in the system. At this time, continuing to increase transportation tasks is conducive to reducing the unit transportation cost, showing good economic effects. When the coefficient is greater than 1, it means that the unit cost rises with the increase in transportation demand, and the system exceeds the optimal load state. Through this indicator, it is possible to describe the impact of demand growth on total cost in different load states of the system.

And the result is in Table 3 and presented in Figure 2.

Table 3. Demand sensitivity analysis.

E	Port-Tug	Dem	Cost	ε
1	8–35	77	14,787.1	–
2		84	15,487.8	0.52
3		91	16,159.4	0.52
4		98	16,740.5	0.47
5		105	17,187.4	0.37
6		112	18,202.6	0.88
7		119	18,381.1	0.16
8		126	19,406.9	0.95
9		133	20,137.0	0.67
10		140	22,549.6	2.27

https://doi.org/10.53941/ijtlr.2026.100006

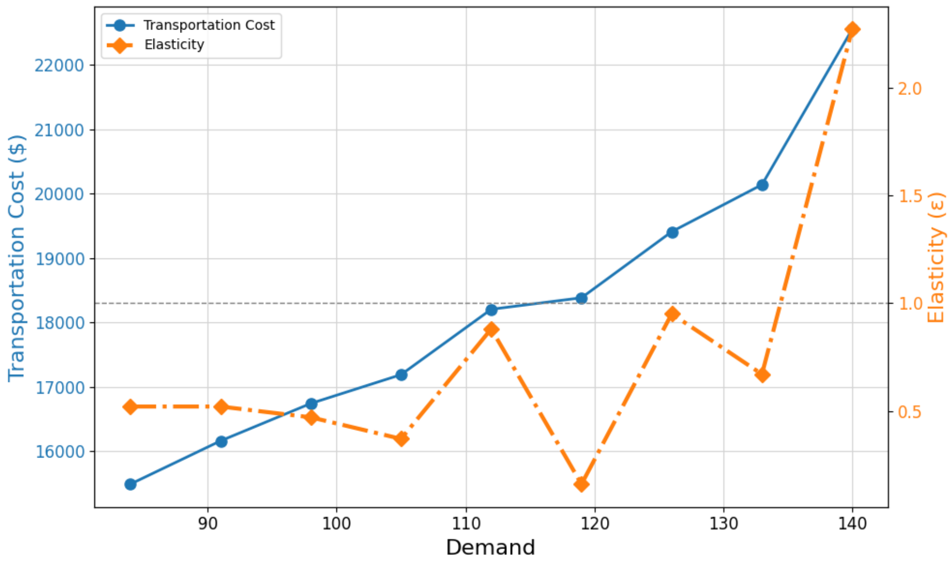

Figure 2. Cost and elasticity analysis in long-distance transportation.

According to the evolutionary characteristics of the cost elasticity (ε), the demand-cost relationship can be divided into three stages:

When Dem ranges from 77 to 105, it marks the first stage. From Figure 2, we can find that transportation costs rise slowly, with ε remaining below 1 and averaging only 0.47. The fluctuation of ε is minimal, and when demand grows within this range, the unit cost of barge transportation declines steadily. In this scenario, the overall load of the system is low, most of the activated tugboats have not reached their towing capacity limits. So, over half of the increased transportation demand is absorbed by existing routes. The optimal transport routes only undergo minor adjustments to accommodate demand growth, indicating that the system is far from reaching its carrying threshold and still possesses substantial transportation potential.

When Dem increases from 105 to 133, it enters the second stage. In this phase, cost increments fluctuate, with significant volatility in ε values whose peaks gradually approach 1, indicating that continuous demand growth can still drive down the unit transportation cost. However, as demand climbs, the carrying capacity of existing routes to absorb new demand gradually weakens. To meet all new demand, more transport routes are put into use, leading to an accelerated cost growth rate. While new routes digest the increased demand, they also release greater transportation capacity. At this point, if demand continues to rise, the degree of change in the route structure tends to moderate. For example, a new route emerges when demand increases to 112, and when demand rises to 119, the new route fully absorbs the subsequent 7 units of demand increment without further route changes, resulting in an ε value of only 0.16 for this stage.

When Dem reaches 140, the third stage begins. Here, transportation costs surge abruptly, with ε undergoing a sudden shift to values far exceeding 1. This indicates that unit costs start to rise instead of falling, meaning further demand growth no longer enjoys the advantages of economies of scale. In terms of optimal tugboat transport routes, when demand hits 140, existing routes can no longer meet new demand at all. The entire transport route structure undergoes radical changes, leading to a sharp increase in the overall complexity of the transportation network and a substantial spike in transportation costs.

5.2.2. Impact of Transportation Cost

This section conducts a sensitivity analysis of cost parameters, focusing on investigating the impact mechanisms of barge carrying cost (CB) and unit transportation cost (CT) on system-wide optimal solutions within their fluctuation ranges. Adopting a dual-variable controlled experimental design framework: the first group was configured with baseline parameter CB = 2, while the second group employed CB = 5, using a baseline demand of 140 shipment uni and keeping 8 ports with a fixed maritime resource conditions (35 tugboats) in this instance. Under the principle of maintaining cost structure comparability and keep a stable CB level, we implemented a gradient ascent strategy for CT: change it from CNY 3 thousand per hour to 7 thousand with step size 0.5. Through systematically observing the rate of change in objective values, this study reveals dynamic impact mechanisms of cost parameter interactions on global optimization targets. Experimental data are presented in Table 4.

This section reveals the variation characteristics of the optimal total cost under the interaction between the tugboat transportation cost (CT) and the unit barge transportation cost (CB) through sensitivity analysis.

The Table 4 shows that when the barge transportation cost (CB) remains at a low level (CB = 2), the increase in tugboat transportation cost (CT) leads to a constant optimal cost increment of 999.33. Analysis of the optimal path under this condition reveals that its structure remains completely unchanged during CT growth. This indicates that the cost increment is determined by the product of the CT increment and the total tugboat operation time on the optimal path, which is a fixed value in this scenario.

Table 4. Comparison of two barge cost environments.

CB	CT	Cost	Δ	CB	CT	Cost	Δ
	3	12,938.76	–		3	23,288.16	–
	3.5	13,938.09	999.33		3.5	24,291.02	1002.86
	4	14,937.42	999.33		4	25,292.86	1001.84
	4.5	15,936.75	999.33		4.5	26,292.19	999.33
2	5	16,936.08	999.33	5	5	27,291.52	999.33
	5.5	17,935.41	999.33		5.5	28,290.85	999.33
	6	18,934.74	999.33		6	29,290.18	999.33
	6.5	19,934.07	999.33		6.5	30,289.51	999.33
	7	20,933.40	999.33		7	31,288.84	999.33

Δ represents the difference between two adjacent obj.

However, when CB increases to a higher level (CB = 5), the initial optimal cost increment from CT = 3 is 1002.86, higher than 999.33. As CT continues to grow, according to Figure 3, these two curves of cost in different CB values in (a) are almost parallel, and the Increment curves in (b) finally become a constant value 999.33. Comparing optimal paths at different CT values, it shows that in high-CB scenarios, the initially lower CT level prompts the optimal solution to introduce an extremely limited path dispersion strategy at the transportation end. This strategy, as can be seen from Figure 4, slightly increases tugboat operation time to save barge time, leading to a higher initial increment.

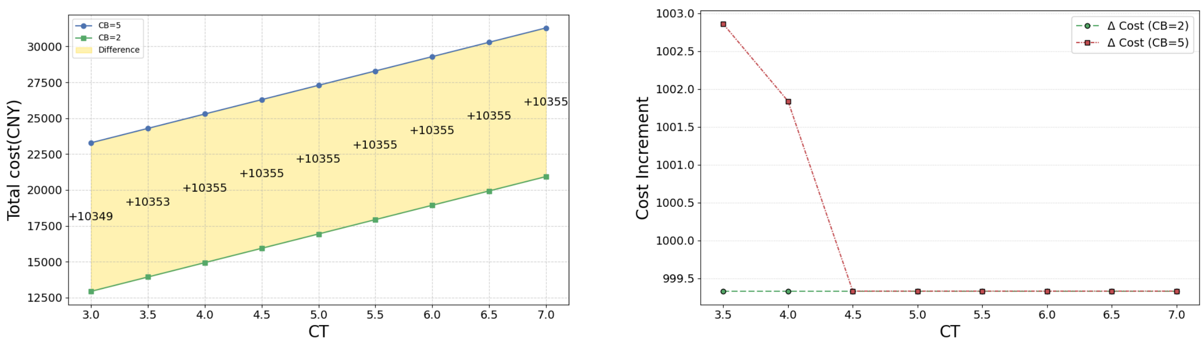

(a) Variation in total cost **(b)** Variation in cost increment

Figure 3. The change of total cost and cost increment under two CB values

It should be noted that highly dispersed paths are inherently inefficient. As shown in Figure 4, the core advantage of drop-and-pull transportation lies in aggregated shipping—tugboats hauling multiple barges with different destinations in a single trip, significantly reducing overall navigation distance to cut costs and improve efficiency. Therefore, only under the specific condition of high barge costs and low tugboat fees may the optimal solution include minimal dispersion at the end to save expensive barge time. Such dispersion is extremely limited, and in the real long-distance tugboat transportation, tugboat fees are usually insufficient to trigger this relatively inefficient strategy. As CT rises, the marginal benefit of saving barge time is quickly offset by increased tugboat costs, and the system reverts to the constant-increment aggregated transportation path, reaffirming the significant cost-efficiency advantage of drop-and-pull transportation.

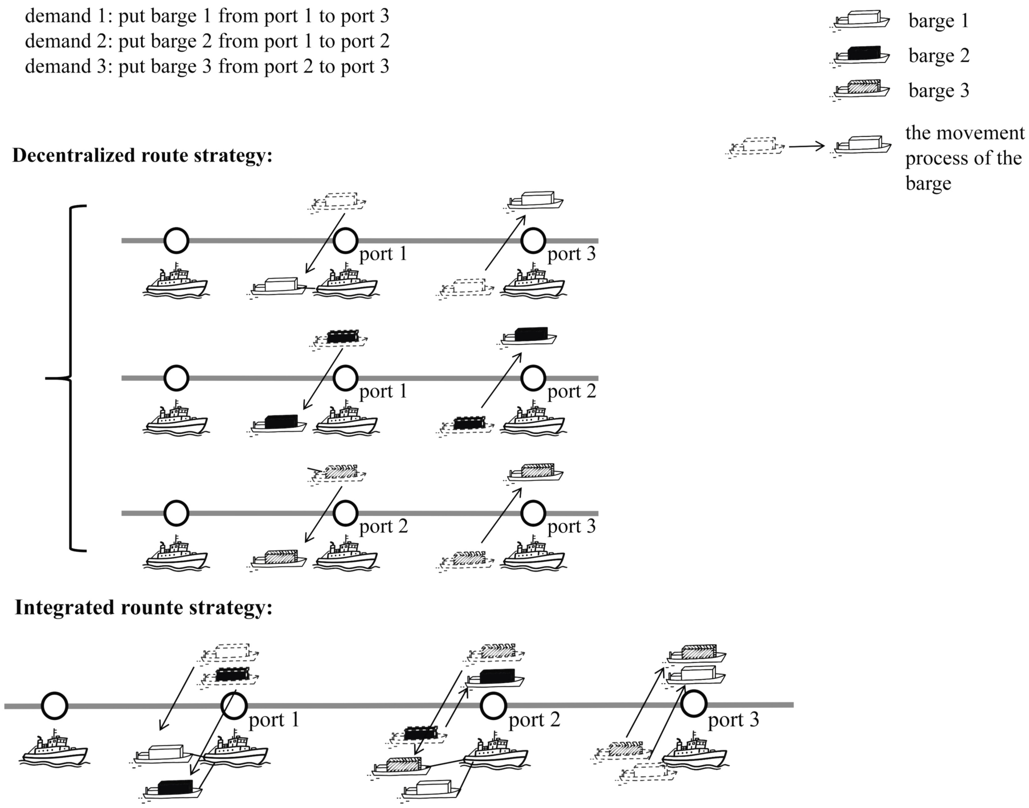

Figure 4. Two strategies.

5.3. Case Study of Short-Distance Shipping

Data description for the regional case study. The short-distance regional network is constructed around Shanghai Port using data from the China Port Yearbook (2023 Edition) [23]. Besides Shanghai, we include three nearby ports with strong barge connections in the lower Yangtze region: Ningbo–Zhoushan, Nantong, and Taicang. The longest sailing leg in this four-port network is the connection between Ningbo–Zhoushan and eastern Nantong, whose distance and typical convoy speed imply a sailing time of roughly 8 h. The planning horizon of this regional system is set to 72 h.

Demand time windows are generated in a manner analogous to the trunk-line case, but with shorter temporal scales: the start of each pickup window is drawn uniformly from $[0, 72 - w_d]$ with window width w_d sampled from $[3, 12]$ h, and delivery windows are obtained by adding sailing times plus a slack of 2–6 h. This configuration captures the high-frequency, short-cycle characteristics of regional barge flows around Shanghai.

Operational constraints are aligned with those in the trunk-line case to facilitate comparison. Each tugboat can tow up to 6 barges, reflecting the regulatory upper bound in the lower Yangtze reaches, and we adopt the same baseline cost parameters as in the long-distance case study. Through comparative analysis with the long-haul trunk-line shipping network, this regional case highlights structural differences in fleet scheduling, resource allocation, and operational patterns across different spatial scales of inland waterway systems.

5.3.1. Impact of Demands

This section designs experiments following Section 5.2, assuming the presence of 16 tugboats operating in a drop and pull transportation mode within the network. The study examines demand variation patterns in the lower Yangtze River transportation network and compares the results with those of the Yangtze River trunkline shipping network. And the outcome is in Table 5.

As can be seen from Figure 5, in the short-distance shipping network, when the demand increases, the total cost still shows a continuous upward trend. However, the cost elasticity coefficient ε does not exhibit a clear three-stage division or a surge in the critical state.

Table 5. Demand sensitivity analysis.

E	Port-Tug	Dem	Cost	ε
1		45	1094.88	–
2		50	1212.53	0.97
3		55	1306.61	0.78
4		60	1340.66	0.29
5	4–16	65	1466.85	1.13
6		70	1565.62	0.88
7		75	1693.16	1.14
8		80	1876.98	1.63
9		85	2056.68	1.53
10		90	——	——

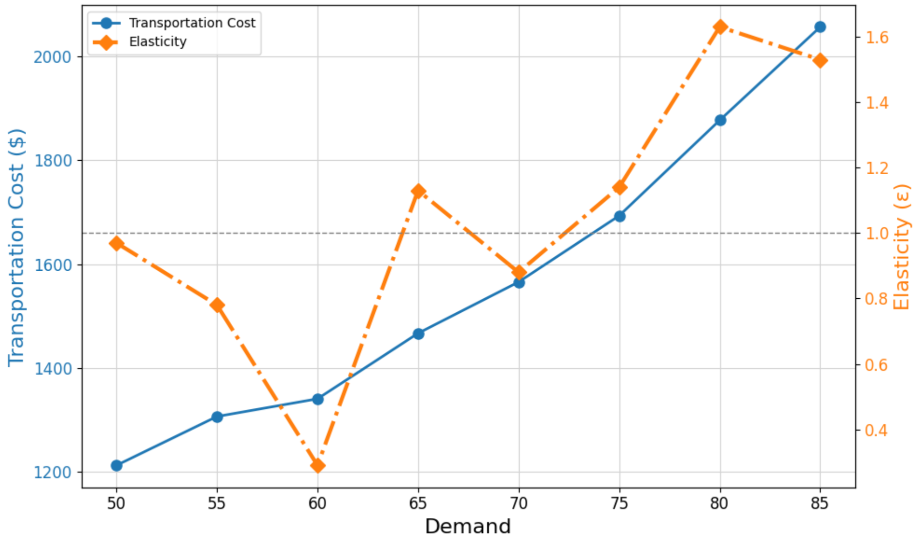

Figure 5. Cost and elasticity analysis in short-distance transportation.

In this scenario, ε fluctuates drastically, similar to the situation in the second stage of Section 5.2. Through analysis of the 9 groups of experiments with optimal feasible solutions, significant variations in the optimal transportation routes were observed. Further analysis of demand characteristics and transportation routes revealed that the transportation network structure in this scenario is relatively simplistic, with more concentrated origins and destinations of transportation demands. As a result, even when initial transportation volumes are low, the actual utilization rates of activated tugboats almost reach 80%, and transportation routes generally approach the upper capacity limit. Figure 6 illustrates the number of activated tugboats and their actual utilization rates under different demand conditions.

Figure 6 also facilitates a better understanding that when the demand rises from 55 to 60, there is a steep decline in ε. This occurs because a new tugboat is activated at this point, causing the actual utilization rate of tugboats to drop. In this short-distance transportation system, the increase in demand can still be potentially met without modifying the original route, although the probability has decreased significantly.

After the demand reaches 75, all tugboats have been fully activated, and the actual tugboat utilization rate remains constantly above 80%. ε continues to rise to over 1.5. When the demand scale further increases and strains the regional transportation network's carrying capacity, the system's complexity surges simultaneously in both spatial and temporal dimensions: new routes intersect and overlap with existing ones spatially, while tugboats are repeatedly activated across multiple time periods temporally. This ultimately causes a significant acceleration in both total transportation costs and cost elasticity, as clearly shown in the subsequent transport network diagrams (Figure 7).

In Figure 7, (a) illustrates the usage of arcs between ports as optimal transportation routes when the demand is 45; (b) shows the usage when the demand is 85. The arcs depict transportation paths, with color indicating the frequency of path usage. The darker the shade, the higher the utilization frequency of the path, implying that a more frequent utilization corresponds to a more complex transportation network and higher transportation costs.

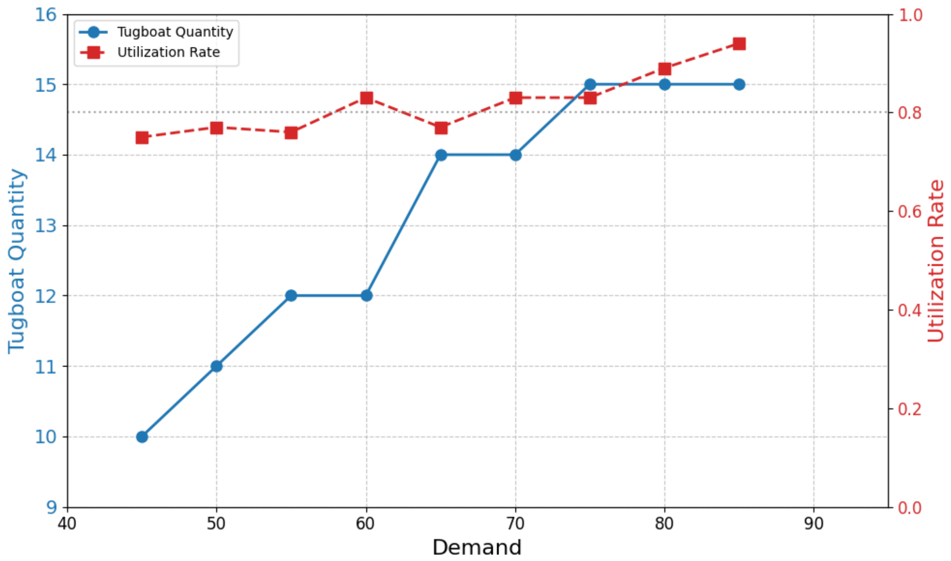

Figure 6. Tugboat quantity and utilization rate vs. demand.

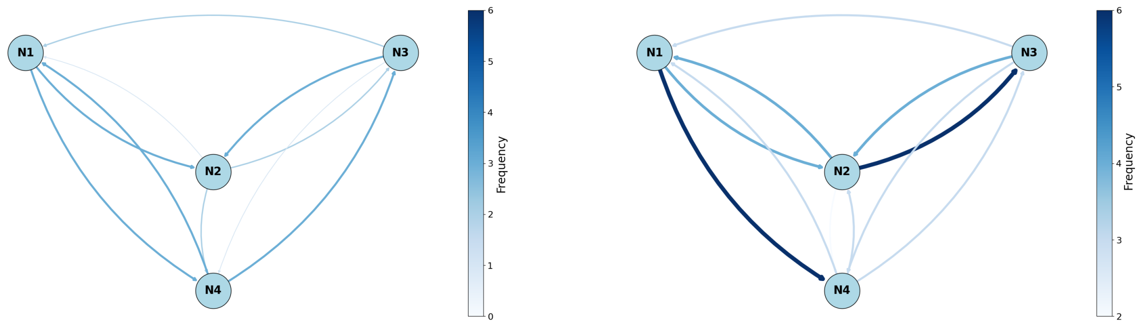

(a) Demand = 45 **(b)** Demand = 85

Figure 7. Comparison of transport networks under different demands.

5.3.2. Impact of Transportation Cost

This section presents the experiment designed with reference to Section 5.2.2 under a small-scale transportation network framework, yielding the following experimental data in Table 6.

Table 6. Comparison of two barge cost environments.

CB	CT	Cost	Δ	CB	CT	Cost	Δ
	3	724.31	–		3	1048.13	–
	3.5	848.17	123.86		3.5	1179.59	131.46
	4	972.03	123.86		4	1311.05	131.46
	4.5	1095.89	123.86		4.5	1442.51	131.46
2	5	1211.34	115.45	5	5	1564.85	122.34
	5.5	1312.50	101.16		5.5	1680.26	115.41
	6	1413.66	101.16		6	1790.32	110.06
	6.5	1514.82	101.16		6.5	1891.48	101.16
	7	1615.98	101.16		7	1992.64	101.16

Δ represents the difference between two adjacent objective values.

It can be seen from the experimental data, that in the short-distance transportation scenario: when CB = 5, two path changes occur, and when CB = 2, one path change occurs, with the routes generally remaining in a stable state. In a high CB level, a lower initial tugboat cost drives paths more disperse to avoid high barge costs. As CT rises, tugboat cost shares grow, amplifying increments from more activated tugs and longer routes. In the low CB value scenario, barge transportation costs have a weaker influence on path selection, and the system tends to adopt a path integration strategy to optimize tug use with gentler cost increases, and hence higher stability. This cost structure difference makes high-CB routes more CT-sensitive, with lower stability than in the other scenario.

What's more, as Figure 8 shows, short-distance optimal paths achieve a 70% tug utilization rate under every transportation demand condition. CT increases can also drive the utilization rate higher through this integration strategy. But once the rate exceeds 80%, the unit cost will show a continuous upward trend, which also prevents the path from undergoing frequent and significant integration changes. When CT increases to 6.5 thousand, the increments under the two barge transportation cost environments eventually become the same. This phenomenon indicates that when CB fluctuates within the range of 2–5, the final optimal route will converge to the same transportation plan.

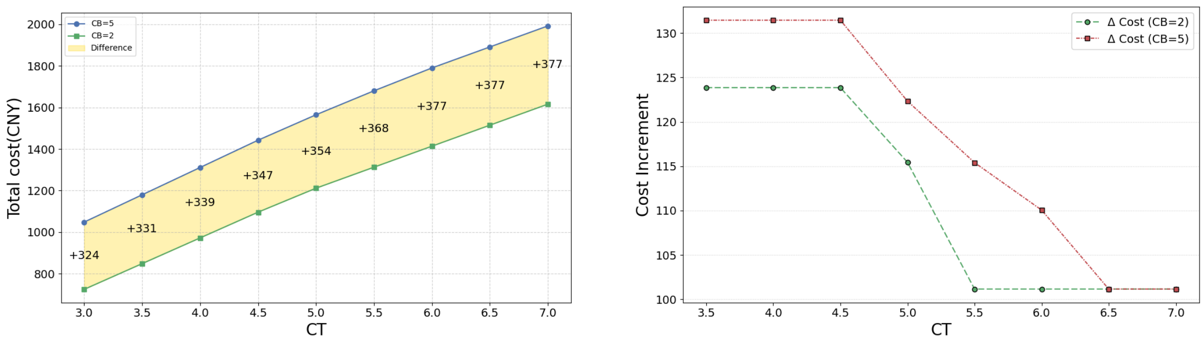

(a) Variation in total cost **(b)** Variation in cost increment

Figure 8. The change of total cost and cost increment in two CB values.

5.4. Managerial Guidance

Beyond the algorithmic and numerical findings, our results also provide managerial insights for a broad range of maritime stakeholders, including barge operators, port authorities, and regulators. In particular, the contrasts between long-distance trunk-line and short-distance regional networks highlight how network structure, demand patterns, and cost parameters jointly shape efficient DP operations and thus inform fleet planning, infrastructure investment, and policy design. According to these analysis, key management implications derived include:

5.4.1. Comparison of Long and Short-distance DP Transport Management

From the perspective of drop-and-pull transportation, long-distance transport focuses on stable inter-regional trunk routes. With complex route planning and high change costs, research shows that optimizing demand allocation and minimizing route changes is key to cost reduction when tug-barge transport costs are stable. In practical situations, given the long haul distances and cycles, operators need to focus on strengthening the supply guarantee of fixed routes, pay attention to demand forecasting, and ensure the load balance of the routes to continuously maintain cost-effectiveness.

On the other hand, short-distance transport serves high-frequency regional terminal distribution with flexible routes. According to the previous results, operators should boost single-route loading efficiency, balance new route costs and revenues during demand surges, and build a shared dispatch network to match idle capacity in real-time for better adaptability to route changes.

5.4.2. The Management Strategy in Different Transport Volume

In the long-distance transportation network with low traffic volume, operators should prioritize meeting new demands without changing existing routes to reduce operating costs. However, continuous increasing of transport demands will lead to a surge in transportation system costs, so it is necessary to closely monitor the cost elasticity index of the system. When the index exceeds 1, capacity input should be timely increased to balance transportation pressure.

In the short-distance transportation network, during the low-traffic phase, scientific scheduling should be adopted to achieve efficient collaborative operations between tugboats and barges, and idle tugboats can be developed for other purposes to reduce resource consumption. In the high-traffic period, according to the experimental results of Section 5.3.1, there is no threshold warning for cost surge in the short-distance transportation network. Therefore, when the system cost elasticity continues to be higher than 1, it is necessary to timely monitor and adjust the ratio of demand to capacity to ensure smooth transportation.

5.4.3. The Management Strategy in Different Transport Cost

The impact of cost fluctuations of barges and tugboats on drop-and-pull transportation management strategies and system operation requires differentiated responses based on the characteristics of transportation distance.

In long-distance drop-and-pull transportation, changes in the costs of barges and tugboats have relatively limited impact on the optimal transportation plan, with the range and frequency of transportation route changes remaining low. Therefore, operators can confirm the transportation fees for barges and tugboats on each route section in advance, reduce the degree of route dispersion to build a more intensive transportation network, prioritize route stability in planning, and even ignore adjustments to optimal plans that only occur in rare cases, so as to ensure the overall efficiency of the transportation network.

For short-distance transportation, cost changes of tugboats and barges will lead to an increase in the frequency of transportation route changes. Given the high inherent flexibility of short-distance transportation routes, operators can pre-plan common transportation routes for different scenarios as pre-arranged plans to prepare for flexible adjustments. Meanwhile, in actual transportation, they can also comprehensively select transportation routes from perspectives such as improving transportation efficiency and reducing wear and tear of transportation equipment, achieving operational optimization through dynamic adjustments.

From a broader maritime perspective, the above insights can assist port authorities in identifying trunk routes and regional corridors that are particularly sensitive to demand growth and cost changes, thereby prioritizing investments in berth capacity, barge terminals, and intermodal connections along these corridors. Regulators and policy makers can use the quantified relationships between cost parameters and routing patterns to evaluate the impact of towing-capacity limits, environmental regulations, or targeted subsidies on both system efficiency and emissions. For shipping lines and logistics integrators, the observed stability of long-distance DP routes versus the flexibility of short-distance operations suggests a hybrid strategy in which stable “backbone” services are complemented by more adaptive regional services, enhancing overall supply chain resilience against demand fluctuations and disruptions.

6. Conclusions

The towing vessel drop-and-pull transportation mode is a relatively novel and efficient water transportation mode in China. Under the DP mode, waiting time primarily originates from time window constraints of transportation demands, which significantly reduces navigation duration, enhances operational efficiency, and achieves notable cost savings. This study investigates cost optimization strategies within this innovative mode, conducting systematic sensitivity analyses on critical parameters to provide managerial insights for different shipping network scenarios. The findings offer quantitative references for fleet deployment and operational management in specific navigation systems such as the middle-lower Yangtze River basin.

However, it should be noted that the mathematical model established in this study still has three limitations: First, the simplified waterway network representation neglects seasonal water-level variations and policy-induced navigational condition fluctuations. Second, the stochastic demand generation mechanism fails to capture spatiotemporal correlations in transportation requirements, particularly the substantial day-night freight volume disparities observed in practice. Third, inherent discrepancies exist between static modeling assumptions and the dynamic nature of actual shipping systems. These constraints suggest that the parameter system needs to be calibrated and corrected according to the characteristics of the port in practical applications.

Subsequent research will focus on breaking through the difficulties of dynamic environment modeling. Shao et al. [25] pointed out that in the actual scenario of truck drop-and-pull transportation, due to the national conditions, one-way transportation is usually adopted in long-distance transportation, which makes drop-and-pull transportation actually uneconomical in long-distance transportation. So it is the same to consider the practical inland water transport demands. Meanwhile, historical freight data will be leveraged to establish demand forecasting models employing convolutional neural networks for detecting holiday-related peak loads and regional cargo flow patterns. Notably, with the application and promotion of new energy vessels, constructing a multi-objective optimization framework covering charging infrastructure planning, battery-swapping cycles, and route scheduling demonstrates potential to advance green shipping initiatives through synergistic resource allocation.

Author Contributions

S.X.: methodology, investigation, formal analysis, software, writing—original draft preparation. X.Q.: conceptualization, supervision, writing—review and editing. Both authors have read and agreed to the published version of the manuscript.

Funding

This work is supported by the National Natural Science Foundation of China (72101223).

Institutional Review Board Statement

Not applicable.

Informed Consent Statement

Not applicable.

Data Availability Statement

Not applicable.

Conflicts of Interest

The authors declare no conflict of interest.

Use of AI and AI-Assisted Technologies

No AI tools were utilized for this paper.

References

1. Wei, X.; Jia, S.; Meng, Q.; et al. Tugboat scheduling for container ports. *Transp. Res. Part E Logist. Transp. Rev.* **2020**, *142*, 102071.
2. Kang, L.; Meng, Q.; Tan, K.C. Tugboat scheduling under ship arrival and tugging process time uncertainty. *Transp. Res. Part E Logist. Transp. Rev.* **2020**, *144*, 102125.
3. Hao, L.; Jin, J.G.; Zhao, K. Joint scheduling of barges and tugboats for river–sea intermodal transport. *Transp. Res. Part E Logist. Transp. Rev.* **2023**, *173*, 103097.
4. Zhen, L.; Wang, K.; Wang, S.; et al. Tug scheduling for hinterland barge transport: A branch-and-price approach. *Eur. J. Oper. Res.* **2018**, *265*, 119–132.
5. Li, B.; Chen, Q.; Lau, Y.Y.; et al. Tugboat scheduling with multiple berthing bases under uncertainty. *J. Mar. Sci. Eng.* **2023**, *11*, 2180.
6. Jia, S.; Li, S.; Lin, X.; et al. Scheduling tugboats in a seaport. *Transp. Sci.* **2021**, *55*, 1370–1391.
7. Xu, Q.; Mao, J.; Jin, Z. Simulated Annealing-Based Ant Colony Algorithm for Tugboat Scheduling Optimization. *Math. Probl. Eng.* **2012**, *2012*, 246978.
8. Sun, C.; Li, M.; Chen, L.; et al. Dynamic tugboat scheduling for large seaports with multiple terminals. *J. Mar. Sci. Eng.* **2024**, *12*, 170.
9. Fan, H.; Zhang, T.H.; Zhao, J.; et al. Berth allocation and tugboat scheduling problem for tidal ports with compound channels: The case of Tianjin port. *Ocean Eng.* **2025**, *324*, 120744.
10. Zhu, S.; Gao, J.; He, X.; et al. Green logistics oriented tug scheduling for inland waterway logistics. *Adv. Eng. Inform.* **2021**, *49*, 101323.
11. Wang, X.; Liang, Y.; Wei, X.; et al. An adaptive large neighborhood search algorithm for the tugboat scheduling problem. *Comput. Ind. Eng.* **2023**, *177*, 109039.
12. Yao, P.; Duan, X.; Tang, J. An improved gray wolf optimization to solve the multi-objective tugboat scheduling problem. *PLoS ONE* **2024**, *19*, e0296966.
13. Ren, Y.; Li, M.; Lei, Y.; et al. Research on tugboat scheduling optimization model considering the reliability of tugboat matching scheme. *Sci. Rep.* **2025**, *15*, 11922.
14. Dumas, Y.; Desrosiers, J.; Soumis, F. The pickup and delivery problem with time windows. *Eur. J. Oper. Res.* **1991**, *54*, 7–22.
15. Li, J.; Geng, Y.; Zhang, L. A Study of Drop and Pull Transport System based on Whole Process Management. *J. Logist. Inf. Serv. Sci* **2014**, *1*, 10–21.
16. Chen, H.; Wang, W.; Cheng, B.; et al. Optimal method for allocation of tractors and trailers in daily dispatches of road drops and pull transport. *J. Adv. Transp.* **2022**, *2022*, 3017196.
17. Shiri, S.; Huynh, N. Optimization of drayage operations with time-window constraints. *Int. J. Prod. Econ.* **2016**, *176*, 7–20.
18. Zhang, R.; Wang, D.; Wang, J. Multi-trailer drop-and-pull container drayage problem. *IEEE Trans. Intell. Transp. Syst.* **2020**, *22*, 5708–5720.
19. Feng, M.; Cheng, Y. Solving truck-cargo matching for drop-and-pull transport with genetic algorithm based on demand-capacity fitness. *Alex. Eng. J.* **2021**, *60*, 61–72.

20. Wang, D.; Moon, I.; Zhang, R. Multi-trip multi-trailer drop-and-pull container drayage problem. *IEEE Trans. Intell. Transp. Syst.* **2022**, *23*, 19088–19104.
21. Wang, D.; Zhang, R.; Qiu, B.; et al. Drop-and-pull container drayage with flexible assignment of work break for vehicle drivers. *Comput. Oper. Res.* **2024**, *162*, 106475.
22. Masson, R.; Lehuédé, F.; Péton, O. An adaptive large neighborhood search for the pickup and delivery problem with transfers. *Transp. Sci.* **2013**, *47*, 344–355.
23. China Ports Association. *China Port Yearbook 2023*; China Ports Association: Shanghai, China, 2023; Volume 476.
24. Oum, T.H.; Yong, J.S. *A Survey of Recent Estimates of Price Elasticities of Demand for Transport*; World Bank Publications: Washington, DC, USA, 1990; Volume 359.
25. Shao, M.; Chen, D.; Lu, X.; et al. Does Drop and Pull Transport Have a Chance? The Case of China. *Sustainability* **2023**, *15*, 10188.